Photocatalytic degradation of bisphenol-A under UV-LED, blacklight and solar irradiation

Photocatalytic degradation of bisphenol-A under UV-LED, blacklight and solar irradiation

K. Davididou[a], R. Nelson[a], J. M. Monteagudo[b], A. Durán[b], A. J. Expósito[b], E. Chatzisymeon[a, *]

[a] School of Engineering, Institute for Infrastructure and Environment, The University of Edinburgh, Edinburgh EH9 3JL, United Kingdom.

[b] Department of Chemical Engineering, Grupo IMAES, Escuela Técnica Superior de Ingenieros Industriales, Instituto de Investigaciones Energéticas y Aplicaciones Industriales (INEI), University of Castilla-La Mancha, Avda. Camilo José Cela 3, 13071 Ciudad Real, Spain.

*Corresponding author: E-mail: e.chatzisymeon@ed.ac.uk; Tel.: +44 1316505711

Abstract

This study aims at investigating the photocatalytic treatment of bisphenol-A (BPA) under various irradiation sources in order to identify cleaner and more sustainable technologies compared to conventional photocatalytic wastewater treatment systems. For this purpose, parallel experimental runs were carried out in two batch-operated slurry photoreactors under UVA irradiation provided by either a light-emitting diode (UV-LED) or a UV blacklight lamp (UV-BL), as well as in a solar compound parabolic collector (CPC) reactor under natural sunlight. The effect of key operating parameters, such as the initial BPA and TiO_2 concentrations, water matrix, and treatment time, on the efficiency of the three photocatalytic systems was evaluated. The photocatalytic degradation of BPA was found to fit well with the pseudo-first-order kinetic model. BPA removal rate increased with catalyst concentration and with decreasing the initial concentration of BPA. The addition of humic acids was found to be inhibitory for all photocatalytic systems. At the best conditions assayed (C_0= 2.5 mg/L, TiO_2= 250 mg/L), BPA was completely degraded within 20, 30, and 120 min under UV-LED, solar, and UV-BL irradiation, respectively. The corresponding reaction rates were 0.230, 0.151, and 0.025 min^{-1}, and TOC removal was 88, 67, and 33% after 90 min of treatment. In all cases, TiO_2/UV-LED achieved the highest removal efficiency and it was found to be significantly more energy-efficient than the TiO_2/UV-BL system. All in all, LED-driven photocatalysis was found to be advantageous over conventional TiO_2/UV-BL systems in terms of performance and sustainability, and an appropriate alternative to solar photocatalysis in areas where sunlight is inadequate.

Keywords: EDCs; water purification; emerging contaminants; light-emitting diodes; solar CPC; photocatalysis

1 Introduction

Bisphenol-A (BPA), a well-known endocrine disrupting compound (EDC), is an alkylphenol used extensively in the synthesis of polycarbonate polymers and epoxy resins (Deblonde et al., 2011). Due to its heat resistance and elasticity, BPA is found in several products, such as food containers, metal cans, and baby bottles (Giulivo et al., 2016; Rubin, 2011). Changes of the inner temperature and pH of BPA-containing materials result in hydrolysis of the ester bonds of BPA, which subsequently lead to BPA leaching into foods and beverages. Ingested BPA is thought to be absorbed by the gastrointestinal tract and then excreted in urine (Giulivo et al., 2016). Existing conventional wastewater treatment plants (WWTPs) are not typically designed for the treatment of such persistent compounds (Belgiorno et al., 2007; Luo et al., 2014), and therefore BPA escapes intact into the aquatic environment by means of the effluent discharges of WWTPs. As a result, BPA has been extensively detected in influent and effluent of WWTPs, groundwater, surface, and drinking water (Kasprzyk-Hordern et al., 2009; Kleywegt et al., 2011; Loos et al., 2010). Exposure to BPA, even at trace level concentrations, has been found to affect the reproductive system of humans (Li et al., 2010; Meeker et al., 2010), and has been linked to growth, developmental, and reproductive effects on aquatic invertebrates, fishes, amphibians, reptiles, birds, and mammalian wildlife (Flint et al., 2012; Zhang et al., 2016). To this end, new, effective and sustainable treatment methods are required to set a barrier to the release of emerging microcontaminants, such as BPA, into the environment.

TiO_2-mediated photocatalysis has received considerable attention because of its efficiency to eliminate EDCs in water and wastewater (Belgiorno et al., 2007; Dalrymple et al., 2007). Photocatalytic oxidation is initiated upon ultraviolet (UV) illumination of a catalyst, usually TiO_2. Highly reactive species, mainly hydroxyl radicals ($^{\bullet}OH$), are then formed and attack organic pollutants, which are eventually mineralised into CO_2 and inorganic anions (Herrmann, 1999; Malato et al., 2009). Sunlight is a free and plentiful renewable energy that can be also used as an irradiation source to increase process sustainability (Legrini et al., 1993). Solar photocatalysis takes advantage of the near-UV band of the solar spectrum to excite TiO_2 catalysts (Malato et al., 2009). In areas where sunlight is inadequate, artificial irradiation is required for photon generation to supplement the efficiency of traditionally employed conventional blacklight fluorescent (UV-BL) lamps (Tokode et al., 2015). However UV-BL lamps suffer from several drawbacks, such as their low energy efficiency, short lifespan and health and safety issues since they contain toxic mercury gas (Jo and Tayade, 2014). As a consequence, UV-BL photocatalytic applications suffer from high treatment costs and increased environmental impacts (Chatzisymeon et al., 2013; Mahamuni and Adewuyi, 2010). To date, 128 countries have signed the Minamata Convention on Mercury, which aims at the gradual phase-out of mercury-containing products by 2020 (Matafonova and Batoev, 2018). Therefore, sustainable mercury-free UV sources are sought to power photochemical oxidation technologies. In this regard, UV light-emitting diodes (UV-LEDs) can be used as eco-friendly alternatives to UV-BL lamps (Davididou et al., 2018). Key features of LEDs include energy efficiency, extended lifetime, and toxic-free nature (i.e. free of mercury and lead, and absence of gas fill) that can lower the cost and improve process sustainability (Tokode et al., 2015).

Several studies have dealt with the photocatalytic degradation of BPA under conventional UVA, vis-LED, and solar irradiation (Subagio et al., 2010; Tsai et al., 2009; Zacharakis et al., 2013). (Saggioro et al., 2014) compared the removal efficiency of BPA under conventional UVA and solar irradiation in batch and compound parabolic collector (CPC) reactors using TiO_2 P25 suspensions. The authors reported enhanced photocatalytic performance in the solar CPC compared to the batch reactor, ascribing it to the optimized optical design of CPC, which allows the use of both direct and diffuse solar irradiation. The present study investigates the photocatalytic degradation of BPA under UVA irradiation provided by either a UV-LED, UV-BL or natural sunlight in parallel experimental runs. To the best of the authors' knowledge, this is the first time that the efficiency of three different photocatalytic systems is compared under similar experimental conditions (i.e. catalyst concentration, substrate concentration, water matrix). Results of this work will create important scientific knowledge on the kinetic rates of BPA degradation under several irradiation sources and how these can be affected by altering basic operating parameters. The lack of an environmentally friendly and low-cost irradiation source with constant availability of light is the main technical barrier that impedes the large-scale application of TiO_2-mediated photocatalytic water treatment. Therefore, findings of this work can be used as a tool for researchers and water industry to further scale-up the process by using the most suitable irradiation source (or a combination of them) that will enable an effective and sustainable treatment of water and wastewater. Moreover, to the best of the authors' knowledge, degradation of BPA under UVA-LED irradiation in the presence of TiO_2 P25 suspensions has not been reported in the literature yet.

For this purpose, photocatalytic experiments were performed both in batch and CPC reactors in the presence of TiO_2 catalyst. The degradation of BPA was studied with consideration to the potential application of photocatalysis as a final polishing step after secondary treatment in domestic wastewater or drinking water treatment plants. The effect of key operating parameters, such as initial substrate and catalyst concentration, treatment time, and water matrix on photocatalytic performance was evaluated. Furthermore, the three photocatalytic systems were compared in terms of their technical and economic benefits.

2 Materials and Methods

2.1 Materials

Bisphenol-A (BPA; ≥ 99% purity, CAS No. 80-05-7) was purchased from Sigma-Aldrich. Leonardite humic acid (HA) IHSS standard was used. HA stock solution was prepared by dissolving a prescribed amount of HA in 0.1 M NaOH and further diluting it in ultra-pure water (UPW; 18.2 MΩ.cm at 25 °C, ELGA LabWater). Aeroxide TiO_2 P25 (anatase:rutile 80:20, 21 nm primary particle size, 50 ± 15 m^2/g BET surface area), supplied by Evonik Industries, was used as the catalyst.

2.2 Photocatalytic experiments

Experiments under artificial irradiation were performed in batch-operated, slurry photoreactors at lab-scale. For LED-driven photocatalysis, an indium gallium nitride (InGaN) UVA emitter (UV-LED; λ = 365 nm, LZ4-00U600, LED Engin) was employed providing continuous irradiation. The UVA emitter was mounted onto a heat sink (588-SV-LED-176E, Ohmite S Series) to prevent radiant flux decrease due to temperature rise on the diode's surface. The LED assembly was placed above the

reactor and a quartz protective plate was placed between them (Figure 1a). The second irradiation source was a UV low-pressure blacklight fluorescent lamp (UV-BL; PLS G23, Casell Lighting), emitting predominantly at λ = 365 nm. UV-BL was housed in a quartz tube and, for the sake of comparison, positioned on top of the reactor at the same height as the LED assembly (i.e. 8 cm distance between irradiation source and surface of reactant mixture at the beginning of each experiment) (Figure 1b). Both set-ups were covered with aluminium shields to prevent light diffusion out of the reactors and minimise penetration of ambient light. The reactors (250 mL Schott Duran beakers, diameter 7 cm, height 9 cm) provided an illuminated area of 38.5 cm^2. The quartz glasses were UV transparent and used to protect the lamps from water spills. UV-LED and UV-BL irradiation sources were driven by electrical power of 11 W and were connected in series to a DC power supply.

Figure 1. Schematics of (a) UV-LED, (b) UV-BL, and (c) solar CPC reactors.

In a typical run, 150 mL of BPA solution was introduced in the photoreactor and a prescribed amount of catalyst was added. The obtained slurry solution was continuously stirred magnetically at 500 rpm to promote uniform dispersion of catalyst powder and dissolved oxygen. At the beginning of each experiment, the solution was stirred in the dark for 30 min to ensure complete adsorption-desorption equilibrium of BPA on the catalyst surface. After adsorption, the UV light source was switched on (taken as t = 0), initiating the photocatalytic redox reactions. Samples were withdrawn at regular time intervals and filtered through 0.45 μm polyvinylidene fluoride (PVDF) syringe filters (CM Scientific Ltd) to remove catalyst particles and

1 further analysed in terms of their organic content. All experiments were conducted at
2 the inherent pH of BPA solution (~ 6.4), which remained constant during
3 photocatalytic treatment.

4 The photocatalytic experiments under solar irradiation were carried out in a
5 compound parabolic collector (CPC) with 0.25 m^2 total illuminated surface area
6 (Figure 1c), manufactured by Ecosystem S.A. The CPC reactor consisted of 2
7 borosilicate tubes providing an irradiated volume of 2 L, solar reflectors (anodised
8 aluminium with a concentration factor of 1), a continuously stirred tank (1.5 L), a
9 centrifugal recirculation pump (flow rate = 30 L/min), connecting tubes, and valves.
10 The CPC reactor was mounted on a fixed south-facing platform 39º tilted, which was
11 installed in Ciudad Real (Spain). A radiometer (Ecosystem, ACADUS 85), 45º tilted,
12 was used to provide the global (direct + diffuse) UV (200 - 400 nm) radiation data.
13 The light intensity of solar irradiation during the photocatalytic experiments ranged
14 from 25 to 30 W/m^2. At the beginning of each experiment, the BPA-polluted water
15 matrix and the catalyst were added into the continuously stirred tank and pumped
16 through the covered reactor for 30 min. This step was applied to ensure adequate
17 mixing and complete equilibration of adsorption-desorption of BPA onto catalyst
18 surface. The reactor was then uncovered initiating the photocatalytic redox reactions
19 (taken as t = 0). Samples were withdrawn at predetermined times, filtered and
20 analysed, as previously described.

21

22 **2.3 Analytical techniques**

23 BPA concentration in the filtered water samples was measured by a high performance
24 liquid chromatography (HPLC) system (S200 Pump, S225 Autosampler, Perkin

Elmer) coupled with a diode array detector (S200 EP, Perkin Elmer). Separation was performed on a reverse phase C18 analytical column (Luna Phenomenex 5u, 250 x 4.6 mm) in isocratic elution mode (flow rate = 1 mL/min). The mobile phase consisted of 35:65 (v/v) UPW:acetonitrile (Frontistis et al., 2011). The injection volume was 40 μL and the detection wavelength was set at 225 nm.

Mineralisation efficiency was determined by measuring the residual organic concentration by a TOC analyser (Shimadzu TOC-V_{CPH}) in the non-purgeable organic carbon (NPOC) mode.

Light intensity and spectral distribution of UV-LED and UV-BL light sources were acquired by a Labsphere spectral irradiance receiver head (E1000) with a concentrator area of 1 cm^2. The distance between the receiver head and the irradiation source was set at 8 cm, which was equal to the distance between UV-LED or UV-BL and the surface of the reactant mixture. More information about the analysis can be found in (Tsonev et al., 2015). The spectral irradiance of UV-LED relatively to that of UV-BL can be seen in Figure 2. The light intensities of UV-LED and UV-BL were estimated to be 1005 and 22.49 W/m^2, respectively.

Figure 2. The relative spectral irradiance of UV-LED and UV-BL irradiation sources and the action spectra of TiO_2 P25 catalyst (in grey).

2.4 Energy consumption

The energy consumption of UV-LED and UV-BL light sources was estimated using figures-of-merit, developed to evaluate the energy efficiency of electric-energy-driven advanced oxidation processes. (Bolton et al., 2001) introduced the concept of the

electric energy per order, E_{EO}, defined as the energy required for 90% degradation of a pollutant per cubic meter of contaminated water. The E_{EO} (kWh/m^3/order) for a batch-operated photoreactor is calculated by equation (1):

$$E_{EO} = \frac{P \times t \times 1000}{V \times 60 \times \log\left(C_i / C_f\right)} \quad (1)$$

where P (kW) is the power of the irradiation source, t (min) is the irradiation time, V (L) is the volume of the treated effluent, and C_i and C_f (mg/L) are the initial and the final pollutant concentrations.

2.5 UV energy requirement

The UV energy requirement of each photocatalytic system is calculated by equation (2):

$$Q_{UV,n+1} = Q_{UV} + \Delta t_n \cdot \overline{UV}_{G,n+1} \cdot \frac{A_i}{V_T};\ \Delta t_n = t_{n+1} - t_n \quad (2)$$

where Q_{UV} (kJ/L) is the accumulated UV energy per unit of volume, $\overline{UV}_{G,n+1}$ (W/m^2) is the average solar UV radiation (λ < 400 nm) measured between t_{n+1} and t_n, A_i (m^2) is the illuminated area, and V_T (L) is the total volume of the reactor. The calculation of Q_{UV} for the solar CPC reactor was based on the average light intensity measured (i.e. 27.5 W/m^2).

3 Results and Discussion

3.1 Effect of initial BPA concentration

To assess the effect of the initial concentration of BPA on photocatalytic performance, different initial BPA concentrations (2.5 – 10 mg/L) were applied in the presence of 125 mg/L TiO_2. As can be seen in Table 1 and the inset graphs of Figure 3, reaction rates decrease with increasing initial concentrations. For instance, a 4-fold increase of BPA concentration (i.e. from 2.5 to 10 mg/L) results in a 3-fold decrease of the reaction rate (i.e. from 0.021 to 0.007 min^{-1}) during UV-BL photocatalytic treatment. The fact that reaction rate changes proportionally less than the initial concentration of BPA implies a shift from first- to zero-order kinetics [although the pseudo-first-order kinetic model was found to describe well the photocatalytic degradation of BPA]. The plot of the normalised BPA concentration against irradiation time resulted in straight lines with the coefficient of linear regression of data fitting, r^2, ranging from 0.90 to 1.00 (Table 1). From the slopes of the resulting lines, the values of the pseudo-first-order kinetic constant, k, were computed.

The increase of initial BPA concentration resulted in decreased removal efficiencies. In detail, when the initial concentration of BPA increased from 2.5 to 10 mg/L, the degradation rate decreased from 99.9 to 79.7% (k = 0.179 – 0.036 min^{-1}) under UV-LED irradiation, and from 66.8 to 29.5% (k = 0.021 – 0.007 min^{-1}) under UV-BL irradiation (Figures 3a and 3b). Similarly, the gradual increase of initial BPA concentration (up to 10 mg/L) decreased its removal efficiency from 99.9 to 72.9% (k = 0.132 – 0.035 min^{-1}) in the CPC reactor (Figure 3c). It is generally accepted that increase in the initial organic concentration, at a fixed set of photocatalytic conditions, lowers the ratio of oxidant species to substrate molecules and further results in decreased degradation yields (Dimitrakopoulou et al., 2012), thus explaining the

findings presented above. According to the results, TiO_2/UV-LED and TiO_2/solar systems could degrade up to 8 and 7.2 mg/L BPA within 45 min of treatment, whereas the respective removal for TiO_2/UV-BL system was limited to 2.9 mg/L.

Figure 3. Effect of initial BPA concentration on photocatalytic degradation under (a) UV-LED, (b) UV-BL, and (c) solar irradiation. Inset graphs: relationship between reaction rate constant and initial BPA concentration (TiO_2 = 125 mg/L).

Table 1. Removal percentages (R), pseudo-first-order kinetic constants (*k*), and coefficients of linear regression of data fitting (r^2) for the photocatalytic degradation of BPA under UV-LED, UV-BL, and solar irradiation.

3.2 Effect of catalyst concentration

Control experiments (i.e. photolysis and catalysis in the dark) were performed to assess the effect of the presence of the catalyst on process efficiency. As can be seen in Figure 4, BPA degradation is negligible after 45 min for both photolysis and catalysis in the dark in TiO_2/UV-LED and TiO_2/UV-BL systems, proving that photocatalysis is the main mechanism for BPA removal. The maximum UV absorbance of BPA appears at 199 and 276 nm, therefore BPA cannot be photolyzed by either UV-LED or UV-BL, which both emit predominantly at 365 nm. Furthermore, existence of UV light ($\lambda < 380$ nm) is a prerequisite for the activation of TiO_2 catalyst, thus explaining the stability of BPA during catalysis in the dark. In the case of solar photolysis and catalysis in the dark, BPA degradation of about 20% was

observed after 45 min of treatment. In the CPC reactor, the borosilicate glass has a cut-off around 285 nm (Malato et al., 2009), however BPA is still photolyzed under solar irradiation at $\lambda \geq 285$ nm since this range falls within the absorbance spectrum of BPA. The experiments in the CPC reactor were performed outdoors and the penetration of ambient light during catalysis in the dark was higher than in the batch reactors, which were placed indoors; a fact that explains the difference in BPA removal between the three systems as can be seen in Figure 4.

The effect of catalyst concentration on process efficiency was then investigated by applying various catalyst concentrations (100 – 500 mg/L) in order to remove 5 mg/L initial BPA concentration. In Figure 4, it is shown that increase of catalyst concentration from 100 to 250 mg/L improves significantly the removal of BPA in TiO_2/UV-LED and TiO_2/solar systems. For instance, the increase of TiO_2 from 100 to 250 mg/L enhances BPA degradation by 21% and doubles the reaction rate (i.e. from 0.040 to 0.080 min^{-1}) in the CPC reactor (Figure 4c, Table 1). However, in TiO_2/UV-BL system, a 4-fold increase of TiO_2 (i.e. from 125 to 500 mg/L) increases the reaction rate only by 1.5 times (i.e. from 0.013 to 0.018 min^{-1}), resulting finally in 64.8% BPA removal after 45 min of treatment [a percentage still much lower than those obtained by TiO_2/UV-LED and TiO_2/solar systems at the half TiO_2 concentration (i.e. 250 mg/L)]. In general, increase of TiO_2 concentration up to a point, where all catalyst particles are totally irradiated, enhances removal efficiency by offering more active sites for photocatalytic oxidation (Kaneco et al., 2004). However, this dependence is less profound in the case of TiO_2/UV-BL system, which can be attributed to the lower light intensity emitted by the UV-BL lamp.

Figure 4. Control experiments and effect of catalyst concentration on photocatalytic degradation under (a) UV-LED, (b) UV-BL, and (c) solar irradiation (C_0 = 5 mg/L).

3.3 Mineralisation efficiency

The aim of photocatalytic oxidation is to destroy both parent compounds, and transformation products (TPs) formed during treatment. To this end, additional experiments were performed at the best-assayed conditions (i.e. C_0 = 2.5 mg/L, TiO_2 = 250 mg/L) to assess the mineralisation efficiency of the three photocatalytic systems. As can be seen in Figure 5, the mineralisation of BPA proceeds slower than BPA degradation, which is attributed to the fact that mineralisation includes a sequence of reactions for the oxidation of BPA and its TPs to CO_2 and H_2O, thus taking longer than the partial oxidation of BPA. In detail, 99.9% of BPA is degraded within 20, 30, and 120 min under UV-LED, solar, and UV-BL irradiation, while the respective TOC removals after 90 min of treatment are 88, 67, and 33%.

Figure 5. BPA and TOC removal under UV-LED, UV-BL, and solar irradiation (C_0 = 2.5 mg/L, TiO_2 = 250 mg/L).

(Kondrakov et al., 2014) reported that the TiO_2-mediated photocatalytic oxidation of BPA is driven by photogenerated holes and hydroxyl radicals leading to the formation of seven TPs according to the mechanism illustrated in Figure 6. Briefly, BPA oxidation proceeds via hydroxylation yielding hydroxylated and oxidized TPs that are transformed into aliphatic alcohols, carboxylic acids, and aldehydes via ring-opening

and further oxidation reactions, before their complete mineralisation (Kondrakov et al., 2014; Repousi et al., 2017).

Figure 6. Mechanism of BPA degradation by TiO_2-mediated photocatalysis, adopted from (Kondrakov et al., 2014).

3.4 Effect of water matrix

Humic acids (HA) solution was used in order to resemble more realistic water and wastewater treatment conditions. HA typically found in surface waters, may interfere with the reactive oxygen species produced during photocatalytic oxidation reactions, and, thus affect the degradation yields. The concentration of HA in surface waters typically varies from 2 to 10 mg/L (Alrousan et al., 2009). Taking this into account, 5 and 8 mg/L HA were added to the reactant mixture to examine the effect of water matrix on the photocatalytic removal of BPA. Noticeably, and as shown in Figure 7, the addition of HA has a detrimental effect on photocatalytic performance under both UV-LED and UV-BL irradiation. Removal efficiency substantially decreases with the increasing concentration of HA. For example, when the reactant mixture is spiked with 8 mg/L HA, BPA removal is suppressed by 77 and 67% under UV-LED and UV-BL irradiation, respectively (Figure 7a). The retardation effect of HA on process efficiency can be ascribed to: (i) the competitive adsorption of HA onto the active sites of TiO_2 that slows down oxidation either via hydroxyl radical ($^{\bullet}OH$) attack or through direct electron transfer between photogenerated holes (h_{vb}^{+}) and target molecules (Selli et al., 1999), and (ii) the reduced light penetration in the solution (Antonopoulou et al., 2015).

Additional experiments were performed at 2.5 mg/L BPA in the presence of 250 mg/L TiO_2 in the CPC reactor. Likewise, the increase in HA concentration from 5 to 8 mg/L resulted in a gradual decrease of BPA degradation rate, as shown in Figure 7b. These results indicate that the retardation degree of photocatalytic oxidation depends strongly on the complexity of the water matrix. Reaction rate decreases with increasing complexity, therefore, degradation in real water samples (e.g. wastewater, surface water) is expected to be slower due to the presence of constituents that can act as hydroxyl radical scavengers (Zacharakis et al., 2013).

Figure 7. Photocatalytic removal of BPA in the presence of different concentrations of HA under (a) UV-LED and UV-BL and (b) solar irradiation ((a) C_0 = 5 mg/L, TiO_2 = 125 mg/L, (b) C_0 = 2.5 mg/L, TiO_2 = 250 mg/L).

3.5 Comparison of the three photocatalytic systems

It was observed that the LED-driven photocatalytic system achieved the highest oxidation reaction rates (Table 1) under all experimental conditions assayed, due to the increased light intensity provided by the UV-LED. Although UV-LED and UV-BL light sources are both driven by the same electrical power of 11 W and emit irradiation predominantly at 365 nm, their light intensities vary significantly. The intensity of UV-LED light is 1005 W/m^2, whereas the light intensity of UV-BL is only 22.49 W/m^2. This difference stems from the directionalities of the two light sources; UV-LED produces a directional beam of light so there is no leak of UV light outside the reactor, UV-BL lamp, to the contrary, emits light in all directions, therefore, a fraction of the photons is lost. However, the higher light intensity

provided by the UV-LED does not lead to the analogous improvement of the reaction rates. In fact, the *k* values obtained during LED-photocatalysis are only 4 – 9 times higher than UV-BL, thus suggesting the lower photonic efficiency of the TiO_2/UV-LED system. This can be explained by the dependency of the reaction rate to light intensity: (i) at low light intensities, the rate of photocatalytic reaction increases linearly with the light intensity, (ii) at intermediate light intensities, reaction rate increases with the square foot of the light intensity because separation of electron-hole pairs competes with recombination, and (iii) at high light intensities, reaction rate becomes independent of the light intensity and mass transfer is the main limitation (Herrmann, 1999; Ollis et al., 1991). Therefore, the right balance should be set between removal efficiency of pollutants and energy requirements of the process in order to obtain sustainable and cost-efficient photocatalytic systems. Scaling-up LED-driven photocatalysis can increase the photonic efficiency of the process because the high rate of energy transfer provided by the UV-LED makes the system ideal for the treatment of large volumes of wastewater.

The consumption of electric energy, E_{EO}, in TiO_2/UV-LED system was found to be significantly lower compared to TiO_2/UV-BL (Figure 8), also suggesting the high sustainability of LED-photocatalysis. For instance, at the best-assayed conditions, E_{EO} has been estimated at 7.171 kWh/m^3/order for TiO_2/UV-LED system and 43.067 kWh/m^3/order for TiO_2/UV-BL. This 6-fold difference in E_{EO} values translates into higher treatment cost for the TiO_2/UV-BL system, as well as increased environmental impact due to augmented CO_2 emissions and fossil depletion (Chatzisymeon et al., 2013). (Shie et al., 2008) and (Shie and Pai, 2010) also found that the photocatalytic degradation of indoor air pollutants (e.g. toluene, formaldehyde) under UV-LED irradiation is a process substantially more energy-efficient than using conventional

UV irradiation sources. At this point, it should be also mentioned that the use of conventional UV lamps further increases the environmental impact of the process due to the hazards related to the presence of mercury.

Figure 8. Electric energy per order (E_{EO}) of TiO_2/UV-LED and TiO_2/UV-BL systems for the photocatalytic degradation of various initial concentrations of BPA (TiO_2 = 125 mg/L).

Comparing the three treatment systems, TiO_2/solar delivers the second highest removal efficiency following TiO_2/UV-LED (Table 1), which is due to the fact that TiO_2 is activated by solar light at $\lambda < 380$ nm, which accounts for only about 5% of the solar spectrum. Solar photocatalysis results in higher degradation rates than TiO_2/UV-BL system, which can be explained by the higher intensity of sunlight (i.e. 25 - 30 W/m^2 at $\lambda < 400$ nm) than UV-BL (i.e. 22.5 W/m^2), as well as the optimised geometry of CPC reactors.

The geometry of the photocatalytic reactors affects significantly process efficiency and this can be seen by the UV energy requirement, Q_{uv}, of the three systems. The Q_{uv}, at the best-assayed conditions, for the removal of 99% of BPA was estimated at 30.9 kJ/L, 4.2 kJ/L, and 3.54 kJ/L for TiO_2/UV-LED, TiO_2/UV-BL, and TiO_2/solar system, respectively. TiO_2/solar system requires the lowest UV energy under the studied conditions. Similar results have been reported by (Saggioro et al., 2014) and (Haranaka-Funai et al., 2017), who compared the photocatalytic performance of CPC and batch-operated reactors in the presence of TiO_2 suspensions. Solar CPC reactors have been already optimised and provide a high optical efficiency that allows the use

of direct and diffuse radiation (Saggioro et al., 2014). Meanwhile, LED photocatalysis is an emerging technology and the optimisation of LED reactors is still under investigation.

Overall, high degradation rates combined with significant advantages regarding process economy and environmental safety, make the TiO_2/solar photocatalytic system ideal for water treatment applications in sun-rich areas. For areas with inadequate sunlight, the use of LEDs as irradiation source was found to be an appropriate alternative to conventional UV-BL lamps, leading to photocatalytic systems of increased performance, energy efficiency and environmental sustainability.

4 Conclusions

The degradation of bisphenol-A (BPA), a well-known endocrine disruptor, was investigated in three photocatalytic systems under various UVA irradiation sources, namely UV-LED, UV-BL lamp, and natural sunlight. The effect of key operating parameters, such as initial BPA, catalyst concentration, treatment time, and water matrix, on the photocatalytic performance of the three systems was assessed. LED-driven photocatalysis yielded the highest reaction rates, followed by TiO_2/solar, and TiO_2/UV-BL systems, under all experimental conditions assayed. UV energy requirements of the three systems was found to descend in the order: TiO_2/solar < TiO_2/UV-BL < TiO_2/UV-LED, indicating the low photonic efficiency of the UV-LED system and, thus, highlighting the need for optimised LED photocatalytic reactors.

All in all, photocatalysis powered by either sunlight, a renewable energy, or LEDs, an energy efficient and environmentally friendly light source, features significant advantages regarding the overall sustainability of the process. The increased

performance and environmental safety of LED-photocatalysis make the process ideal for the removal of emerging micropollutants in areas where solar photocatalysis might not be feasible due to inadequate sunlight. LEDs could be also used as a backup irradiation source in solar photocatalytic systems during less sunny days or periods with increased influent loads (e.g. touristic periods). To this end, future work should focus on the evaluation of process efficiency in real secondary wastewater matrices with emerging micropollutants present at environmentally relevant concentrations. Also, economic and environmental impact assessment of LED-photocatalysis is necessary in order to establish the suitability of the process as a tertiary treatment step in WWTPs before further scale-up.

Acknowledgements

Financial support from MINECO (CTM2013-44317-R and CTQ2017-83549-R) is gratefully acknowledged. The authors would also like to thank Dr John Fakidis from Li-Fi R&D Centre at the University of Edinburgh for the measurements of the spectral irradiance of UV-LED and UV-BL.

References

Alrousan, D.M.A., Dunlop, P.S.M., McMurray, T.A., Byrne, J.A., 2009. Photocatalytic inactivation of E. coli in surface water using immobilised nanoparticle TiO2 films. Water Res. 43, 47-54.

Antonopoulou, M., Skoutelis, C.G., Daikopoulos, C., Deligiannakis, Y., Konstantinou, I.K., 2015. Probing the photolytic–photocatalytic degradation mechanism of DEET in the presence of natural or synthetic humic macromolecules using molecular-scavenging techniques and EPR spectroscopy. Journal of Environmental Chemical Engineering 3, 3005-3014.

Belgiorno, V., Rizzo, L., Fatta, D., Della Rocca, C., Lofrano, G., Nikolaou, A., Naddeo, V., Meric, S., 2007. Review on endocrine disrupting-emerging compounds in

urban wastewater: occurrence and removal by photocatalysis and ultrasonic irradiation for wastewater reuse. Desalination 215, 166-176.

Bolton, J.R., Bircher, K.G., Tumas, W., Tolman, C.A., 2001. Figures-of-merit for the technical development and application of advanced oxidation technologies for both electric- and solar-driven systems. Pure Appl. Chem. 73, 627-637.

Chatzisymeon, E., Foteinis, S., Mantzavinos, D., Tsoutsos, T., 2013. Life cycle assessment of advanced oxidation processes for olive mill wastewater treatment. Journal of Cleaner Production 54, 229-234.

Dalrymple, O.K., Yeh, D.H., Trotz, M.A., 2007. Removing pharmaceuticals and endocrine-disrupting compounds from wastewater by photocatalysis. Journal of Chemical Technology & Biotechnology 82, 121-134.

Davididou, K., McRitchie, C., Antonopoulou, M., Konstantinou, I., Chatzisymeon, E., 2018. Photocatalytic degradation of saccharin under UV-LED and blacklight irradiation. Journal of Chemical Technology & Biotechnology 93, 269-276.

Deblonde, T., Cossu-Leguille, C., Hartemann, P., 2011. Emerging pollutants in wastewater: A review of the literature. Int. J. Hyg. Environ. Health 214, 442-448.

Dimitrakopoulou, D., Rethemiotaki, I., Frontistis, Z., Xekoukoulotakis, N.P., Venieri, D., Mantzavinos, D., 2012. Degradation, mineralization and antibiotic inactivation of amoxicillin by UV-A/TiO2 photocatalysis. J. Environ. Manage. 98, 168-174.

Flint, S., Markle, T., Thompson, S., Wallace, E., 2012. Bisphenol A exposure, effects, and policy: A wildlife perspective. J. Environ. Manage. 104, 19-34.

Frontistis, Z., Daskalaki, V.M., Katsaounis, A., Poulios, I., Mantzavinos, D., 2011. Electrochemical enhancement of solar photocatalysis: Degradation of endocrine disruptor bisphenol-A on Ti/TiO2 films. Water Res. 45, 2996-3004.

Giulivo, M., Lopez de Alda, M., Capri, E., Barceló, D., 2016. Human exposure to endocrine disrupting compounds: Their role in reproductive systems, metabolic syndrome and breast cancer. A review. Environ. Res. 151, 251-264.

Haranaka-Funai, D., Didier, F., Giménez, J., Marco, P., Esplugas, S., Machulek-Junior, A., 2017. Photocatalytic treatment of valproic acid sodium salt with TiO2 in different experimental devices: An economic and energetic comparison. Chem. Eng. J. 327, 656-665.

Herrmann, J.-M., 1999. Heterogeneous photocatalysis: fundamentals and applications to the removal of various types of aqueous pollutants. Catal. Today 53, 115-129.

Jo, W.-K., Tayade, R.J., 2014. New Generation Energy-Efficient Light Source for Photocatalysis: LEDs for Environmental Applications. Industrial & Engineering Chemistry Research 53, 2073-2084.

Kaneco, S., Rahman, M.A., Suzuki, T., Katsumata, H., Ohta, K., 2004. Optimization of solar photocatalytic degradation conditions of bisphenol A in water using titanium dioxide. Journal of Photochemistry and Photobiology A: Chemistry 163, 419-424.

Kasprzyk-Hordern, B., Dinsdale, R.M., Guwy, A.J., 2009. The removal of pharmaceuticals, personal care products, endocrine disruptors and illicit drugs during wastewater treatment and its impact on the quality of receiving waters. Water Res. 43, 363-380.

Kleywegt, S., Pileggi, V., Yang, P., Hao, C., Zhao, X., Rocks, C., Thach, S., Cheung, P., Whitehead, B., 2011. Pharmaceuticals, hormones and bisphenol A in untreated source and finished drinking water in Ontario, Canada — Occurrence and treatment efficiency. Sci. Total Environ. 409, 1481-1488.

Kondrakov, A.O., Ignatev, A.N., Frimmel, F.H., Bräse, S., Horn, H., Revelsky, A.I., 2014. Formation of genotoxic quinones during bisphenol A degradation by TiO2 photocatalysis and UV photolysis: A comparative study. Applied Catalysis B: Environmental 160–161, 106-114.

Legrini, O., Oliveros, E., Braun, A.M., 1993. Photochemical processes for water treatment. Chem. Rev. 93, 671-698.

Li, D.K., Zhou, Z., Miao, M., He, Y., Qing, D., Wu, T., Wang, J., Weng, X., Ferber, J., Herrinton, L.J., Zhu, Q., Gao, E., Yuan, W., 2010. Relationship Between Urine Bisphenol-A Level and Declining Male Sexual Function. Journal of Andrology 31, 500-506.

Loos, R., Locoro, G., Comero, S., Contini, S., Schwesig, D., Werres, F., Balsaa, P., Gans, O., Weiss, S., Blaha, L., Bolchi, M., Gawlik, B.M., 2010. Pan-European survey on the occurrence of selected polar organic persistent pollutants in ground water. Water Res. 44, 4115-4126.

Luo, Y., Guo, W., Ngo, H.H., Nghiem, L.D., Hai, F.I., Zhang, J., Liang, S., Wang, X.C., 2014. A review on the occurrence of micropollutants in the aquatic environment and their fate and removal during wastewater treatment. Sci. Total Environ. 473-474, 619-641.

Mahamuni, N.N., Adewuyi, Y.G., 2010. Advanced oxidation processes (AOPs) involving ultrasound for waste water treatment: A review with emphasis on cost estimation. Ultrason. Sonochem. 17, 990-1003.

Malato, S., Fernández-Ibáñez, P., Maldonado, M.I., Blanco, J., Gernjak, W., 2009. Decontamination and disinfection of water by solar photocatalysis: Recent overview and trends. Catal. Today 147, 1-59.

Matafonova, G., Batoev, V., 2018. Recent advances in application of UV light-emitting diodes for degrading organic pollutants in water through advanced oxidation processes: A review. Water Res. 132, 177-189.

Meeker, J.D., Ehrlich, S., Toth, T.L., Wright, D.L., Calafat, A.M., Trisini, A.T., Ye, X., Hauser, R., 2010. Semen quality and sperm DNA damage in relation to urinary bisphenol A among men from an infertility clinic. Reprod. Toxicol. 30, 532-539.

Ollis, D.F., Pelizzetti, E., Serpone, N., 1991. Photocatalyzed destruction of water contaminants. Environ. Sci. Technol. 25, 1522-1529.

1 Repousi, V., Petala, A., Frontistis, Z., Antonopoulou, M., Konstantinou, I.,
2 Kondarides, D.I., Mantzavinos, D., 2017. Photocatalytic degradation of bisphenol A
3 over Rh/TiO2 suspensions in different water matrices. Catal. Today 284, 59-66.

4 Rubin, B.S., 2011. Bisphenol A: An endocrine disruptor with widespread exposure
5 and multiple effects. The Journal of Steroid Biochemistry and Molecular Biology 127,
6 27-34.

7 Saggioro, E.M., Oliveira, A.S., Pavesi, T., Tototzintle, M.J., Maldonado, M.I.,
8 Correia, F.V., Moreira, J.C., 2014. Solar CPC pilot plant photocatalytic degradation of
9 bisphenol A in waters and wastewaters using suspended and supported-TiO2.
10 Influence of photogenerated species. Environmental Science and Pollution Research
11 21, 12112-12121.

12 Selli, E., Baglio, D., Montanarella, L., Bidoglio, G., 1999. Role of humic acids in the
13 TiO2-photocatalyzed degradation of tetrachloroethene in water. Water Res. 33, 1827-
14 1836.

15 Shie, J.-L., Lee, C.-H., Chiou, C.-S., Chang, C.-T., Chang, C.-C., Chang, C.-Y., 2008.
16 Photodegradation kinetics of formaldehyde using light sources of UVA, UVC and
17 UVLED in the presence of composed silver titanium oxide photocatalyst. J. Hazard.
18 Mater. 155, 164-172.

19 Shie, J.-L., Pai, C.-Y., 2010. Photodegradation Kinetics of Toluene in Indoor Air at
20 Different Humidities Using UVA, UVC and UVLED Light Sources in the Presence of
21 Silver Titanium Dioxide. Indoor Built Environ. 19, 503-512.

22 Subagio, D.P., Srinivasan, M., Lim, M., Lim, T.-T., 2010. Photocatalytic degradation
23 of bisphenol-A by nitrogen-doped TiO2 hollow sphere in a vis-LED photoreactor.
24 Applied Catalysis B: Environmental 95, 414-422.

25 Tokode, O., Prabhu, R., Lawton, L., Robertson, P.J., 2015. UV LED Sources for
26 Heterogeneous Photocatalysis, in: Bahnemann, D.W., Robertson, P.K.J. (Eds.),
27 Environmental Photochemistry Part III. Springer Berlin Heidelberg, pp. 159-179.

28 Tsai, W.-T., Lee, M.-K., Su, T.-Y., Chang, Y.-M., 2009. Photodegradation of
29 bisphenol-A in a batch TiO2 suspension reactor. J. Hazard. Mater. 168, 269-275.

30 Tsonev, D., Videv, S., Haas, H., 2015. Towards a 100 Gb/s visible light wireless
31 access network. Opt. Express 23, 1627-1637.

32 Zacharakis, A., Chatzisymeon, E., Binas, V., Frontistis, Z., Venieri, D., Mantzavinos,
33 D., 2013. Solar Photocatalytic Degradation of Bisphenol A on Immobilized ZnO or
34 TiO2. International Journal of Photoenergy 2013, 9.

35 Zhang, C., Li, Y., Wang, C., Niu, L., Cai, W., 2016. Occurrence of endocrine
36 disrupting compounds in aqueous environment and their bacterial degradation: A
37 review. Crit. Rev. Environ. Sci. Technol. 46, 1-59.

38

List of Tables

Table 1. Removal percentages (R), pseudo-first-order kinetic constants (*k*), and coefficients of linear regression of data fitting (r^2) for the photocatalytic degradation of BPA under UV-LED, UV-BL, and solar irradiation.

1

2

3

4

5

6 Table 1.

Operating parameter	Irradiation source	mg/L	R, %	Pseudo-first-order reaction model	
				k, min^{-1}	r^2
C_0[a]	UV-LED	2.5	99.9	0.179	1.00
		5	95.9	0.058	1.00
		7.5	90.6	0.047	0.98
		10	79.7	0.036	0.99
	UV-BL	2.5	66.8	0.021	0.98
		5	45.6	0.013	0.97
		7.5	36.0	0.011	0.99
		10	29.5	0.007	0.98
	Solar	2.5	99.9	0.132	0.95
		5	84.0	0.047	0.93
		7.5	81.5	0.037	0.90
		10	72.9	0.035	0.98
TiO_2[b]	UV-LED	100	97.9	0.068	0.99
		125	95.9	0.057	1.00
		250	99.0	0.101	1.00
	UV-BL	125	45.6	0.013	0.97
		250	57.5	0.016	0.97
		500	64.8	0.018	0.99
	Solar	100	79.0	0.040	0.99
		125	84.0	0.047	0.93
		250	99.9	0.080	0.97
Best-assayed operating conditions[c]	UV-LED		99.9	0.230	0.99
	UV-BL		75.6	0.025	0.98
	Solar		99.9	0.151	0.98

7 [a]TiO_2 = 125 mg/L, irradiation time = 45 min;

[b] C_0 = 5 mg/L, irradiation time = 45 min;
[c] C_0 = 2.5 mg/L, TiO_2 =250 mg/L, irradiation time = 45 min.

List of Figures

Figure 1. Schematics of (a) UV-LED, (b) UV-BL, and (c) solar CPC reactors.

Figure 2. The relative spectral irradiance of UV-LED and UV-BL irradiation sources and the action spectra of TiO_2 P25 catalyst (in grey).

Figure 3. Effect of initial BPA concentration on photocatalytic degradation under (a) UV-LED, (b) UV-BL, and (c) solar irradiation. Inset graphs: relationship between reaction rate constant and initial BPA concentration (TiO_2 = 125 mg/L).

Figure 4. Control experiments and effect of catalyst concentration on photocatalytic degradation under (a) UV-LED, (b) UV-BL, and (c) solar irradiation (C_0 = 5 mg/L).

Figure 5. BPA and TOC removal under UV-LED, UV-BL, and solar irradiation (C_0 = 2.5 mg/L, TiO_2 = 250 mg/L).

Figure 6. Mechanism of BPA degradation by TiO_2-mediated photocatalysis, adopted from (Kondrakov et al., 2014).

Figure 7. Photocatalytic removal of BPA in the presence of different concentrations of HA under (a) UV-LED and UV-BL and (b) solar irradiation ((a) C_0 = 5 mg/L, TiO_2 = 125 mg/L, (b) C_0 = 2.5 mg/L, TiO_2 = 250 mg/L).

Figure 8. Electric energy per order (E_{EO}) for TiO_2/UV-LED and TiO_2/UV-BL systems for the photocatalytic degradation of different initial concentrations of BPA (TiO_2 = 125 mg/L).

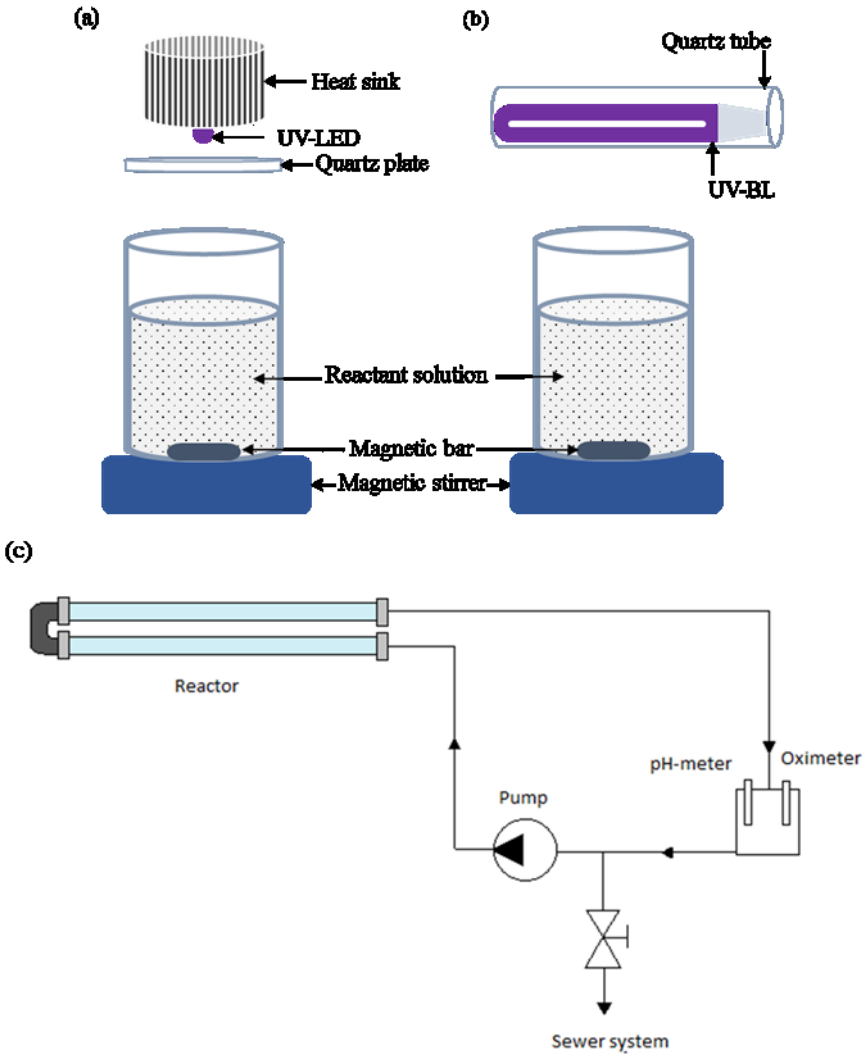

Figure 1. Schematics of (a) UV-LED, (b) UV-BL, and (c) solar CPC reactors.

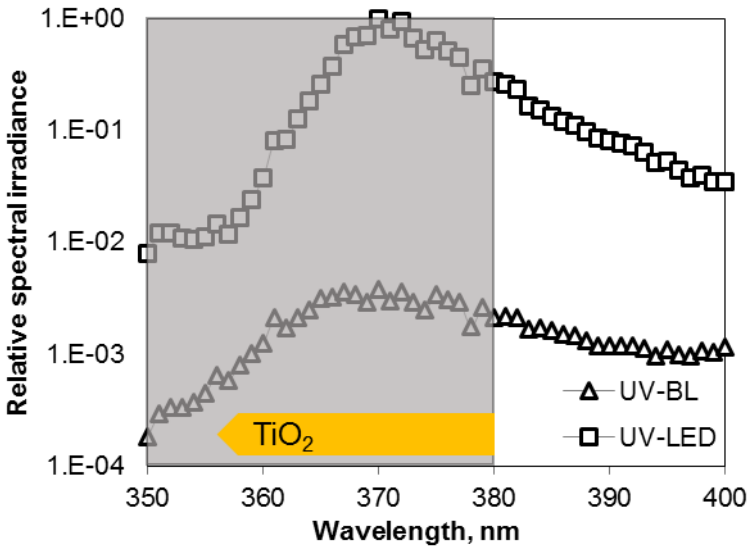

Figure 2. The relative spectral irradiance of UV-LED and UV-BL irradiation sources and the action spectra of TiO_2 P25 catalyst (in grey).

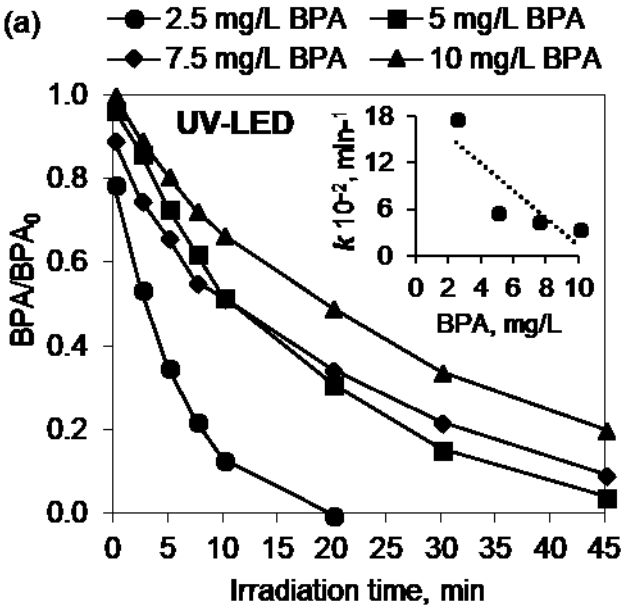
(a)
2.5 mg/L BPA
5 mg/L BPA
7.5 mg/L BPA
10 mg/L BPA
UV-LED
BPA/BPA0
Irradiation time, min
k·10-2, min-1
BPA, mg/L

1

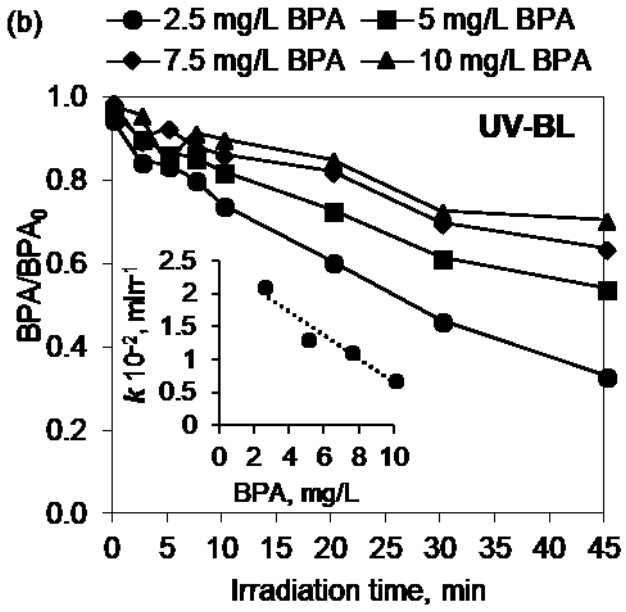
(b)
2.5 mg/L BPA
5 mg/L BPA
7.5 mg/L BPA
10 mg/L BPA
UV-BL
BPA/BPA0
Irradiation time, min
k·10-2, min-1
BPA, mg/L

2

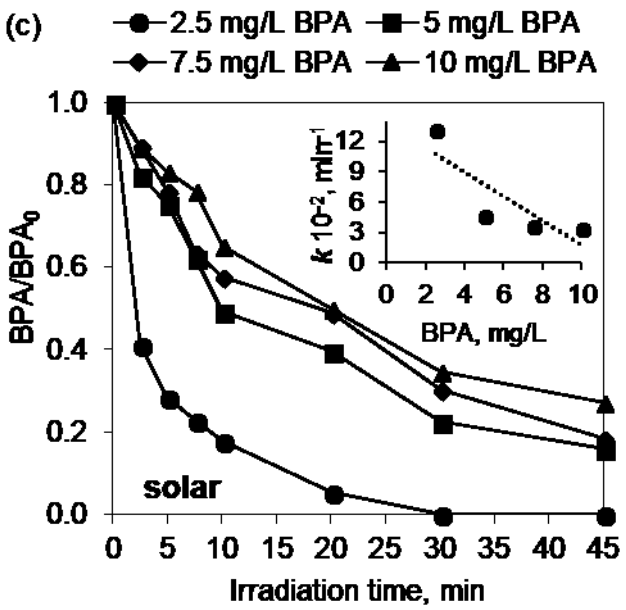

Figure 3. Effect of initial BPA concentration on photocatalytic degradation under (a) UV-LED, (b) UV-BL, and (c) solar irradiation. Inset graphs: relationship between reaction rate constant and initial BPA concentration (TiO_2 = 125 mg/L).

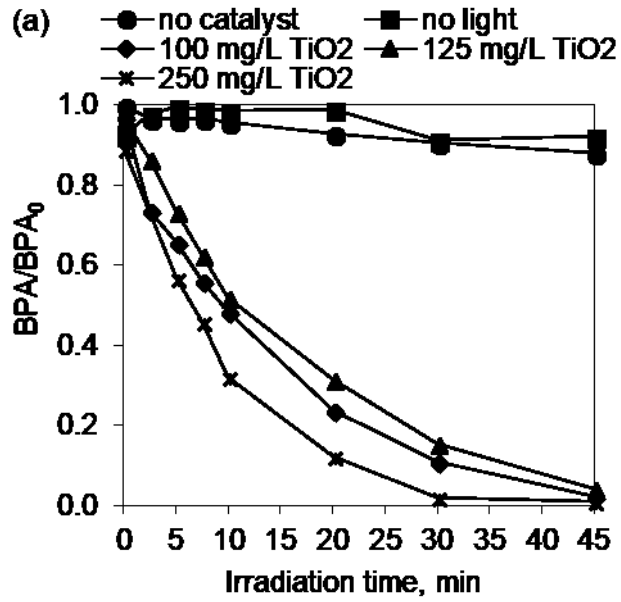
(a)
no catalyst
no light
100 mg/L TiO2
125 mg/L TiO2
250 mg/L TiO2
BPA/BPA0
1.0
0.8
0.6
0.4
0.2
0.0
0 5 10 15 20 25 30 35 40 45
Irradiation time, min

1

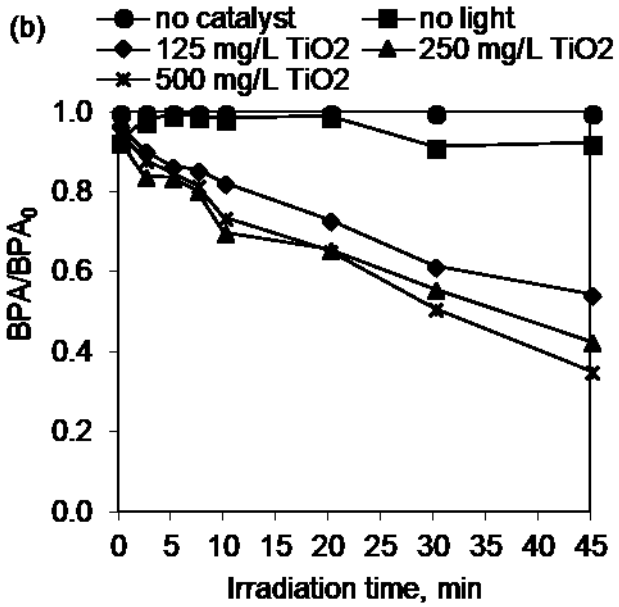
(b)
no catalyst
no light
125 mg/L TiO2
250 mg/L TiO2
500 mg/L TiO2
BPA/BPA0
1.0
0.8
0.6
0.4
0.2
0.0
0 5 10 15 20 25 30 35 40 45
Irradiation time, min

2

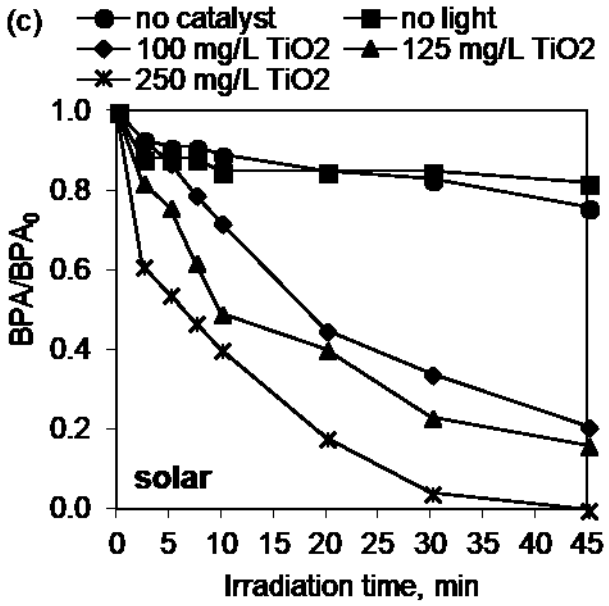

Figure 4. Control experiments and effect of catalyst concentration on photocatalytic degradation under (a) UV-LED, (b) UV-BL, and (c) solar irradiation (C_0 = 5 mg/L).

Figure 5. BPA and TOC removal under UV-LED, UV-BL, and solar irradiation (C_0 = 2.5 mg/L, TiO_2 = 250 mg/L).

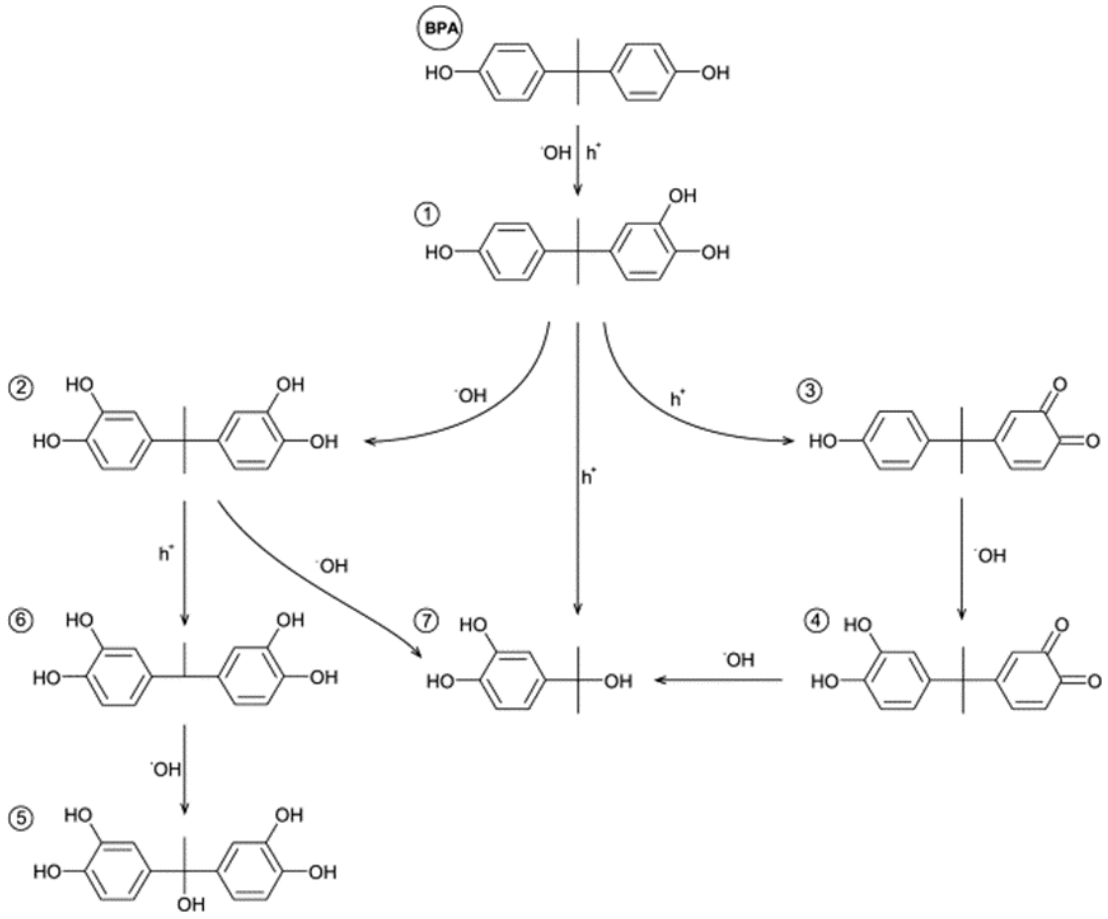

Figure 6. Mechanism of BPA degradation by TiO_2-mediated photocatalysis, adopted from (Kondrakov et al., 2014).

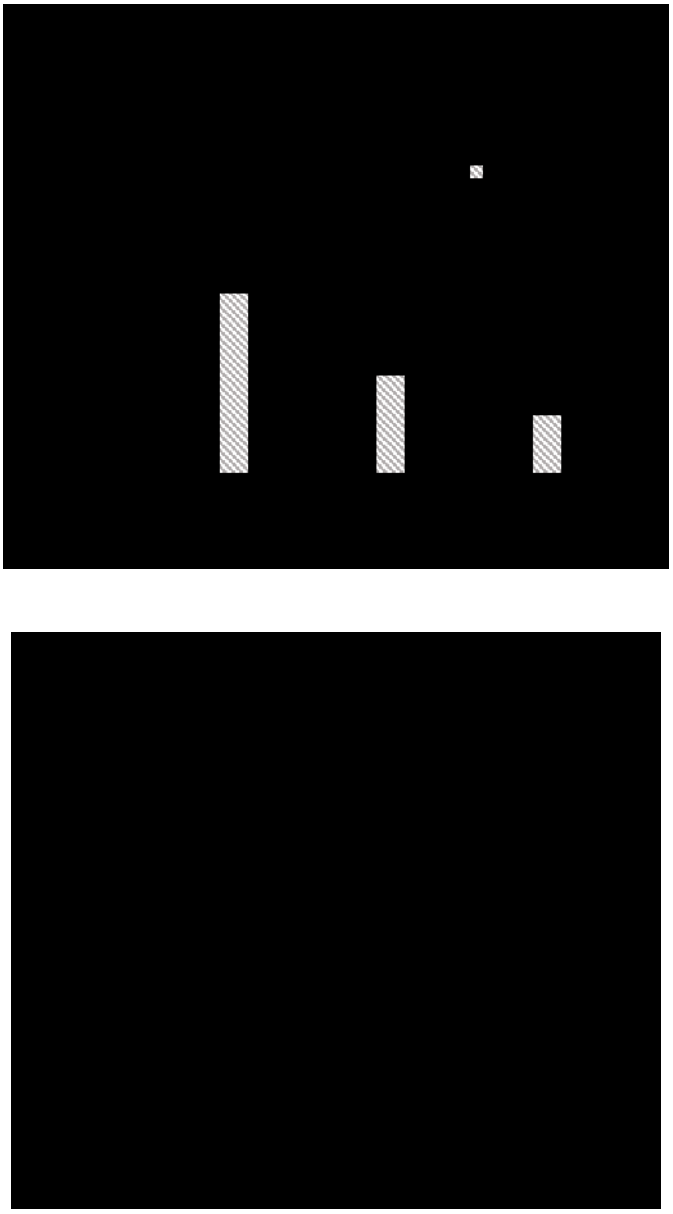

Figure 7. Photocatalytic removal of BPA in the presence of different concentrations of HA under (a) UV-LED and UV-BL and (b) solar irradiation ((a) C_0 = 5 mg/L, TiO_2 = 125 mg/L, (b) C_0 = 2.5 mg/L, TiO_2 = 250 mg/L).

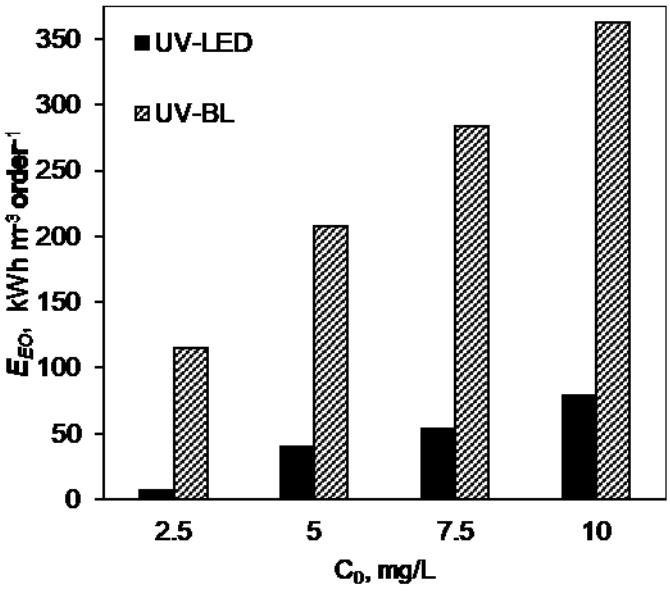

Figure 8. Electric energy per order (E_{EO}) of TiO_2/UV-LED and TiO_2/UV-BL systems for the photocatalytic degradation of different initial concentrations of BPA (TiO_2 = 125 mg/L).